

# CHAPTR ONE

## Introduction

### 1.1 Background

One of the most important residues in the sugar crop farms that are produced from the extraction of ethanol is Vinasse, which is a liquid produced by the process of fermentation of molasses for the production of alcohol and various yeasts, and has attraotal the attention of scientists to try to save cleanliness Environment.(omima,2010)

Vinasse are produced during the process of fermentation and distillation of molasses for the production of ethanol, which is produced in large quantities based on the quality of molasses ranging from 12 to 20 liters versus 1 liter of pure alcohol..(omima,2010)

Vinasse are used after anaerobic digestion by bacteria and then burned by large kilns to produce potassium-rich fertilizer and used for soil fertilization. (omima,2010)

### 1.2 Research Problem

Vinasse is considered to be an extractable substance and a soil-damaging substance where the soil will lose its fertility after five years. So this work trying to extract a useful material from Vinasse by process it by laser.

### 1.3 The Goal of the Research

- convert the residues of the sugar crop into a valuable material, throw the burning of vinasse by laser.

- examining the produced material after burning and analyzing it.
- find a new way to benefit from the substance of phoenix.

## **1.4 Research Methodology**

Vinasse will be burned by Nd-YAG laser with a 60 Watt power for 50 seconds to transform the vinasse from a damp paste into a powder and then tested by XRF, XRD and FTIR.

## **1.5 Dissertation Layout**

This dissertation consists of four chapters; the first one concerns the background and introduction. In the second chapter contains the theoretical background, the data information of the samples used in the sampling of x-ray fluorescence, x-ray diffraction and Fourier-transform Infrared Spectroscopy. The experimental work about the preparation of the sample and the method of burning it with laser and characterizations will be in chapter three. In the fourth chapter shows the findings, discussions and how to benefit from the resulting material. Finally, the list of references.

# CHAPTER TWO

## Theoretical Background

### 2.1 Laser

"Light Amplification by Stimulated Emission of Radiation"

This is a bit of a misnomer. A laser is actually an oscillator rather than a simple amplifier.

The difference is that an oscillator has positive feedback in addition to the amplifier (Wu,2009).

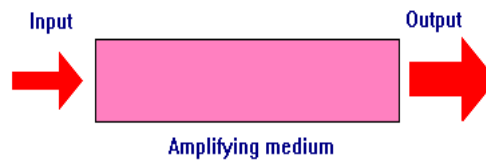


Figure 2.1: Amplification of light(Wu,2009).

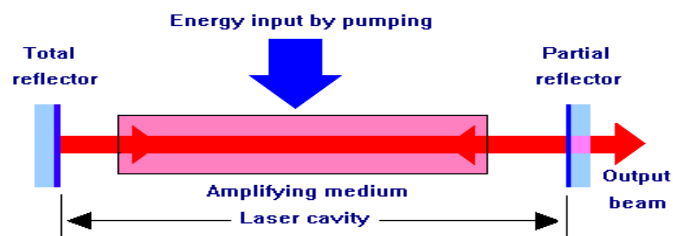


Figure 2.2: A Laser Device(Wu,2009).

#### 2.1.1 Kinds of Lasers

Lasers can be divided into groups according to different criteria:

1. The state of matter of the active medium:

Solid, liquid, gas, or plasma.

2. The spectral range of the laser Wavelength: visible spectrum, Infra-Red(IR) spectrum, etc.

3. The excitation (pumping) method of the active medium: Optical pumping, Electrical, Pumping, etc.

4. The characteristics of the radiation emitted from the laser. CW mode or pulsed mode, temporal distribution, spatial distribution, etc (Wu,2009).

## 2.1.2 Properties of Laser Light

1- Monochromaticity

2- Directionality

3 - Brightness

4 - Coherence

### 2.1.2.1 Monochromaticity

Monochromaticity means "One color".

When "white light" is transmitted through a prism, it is divided into the different colors which are in it.

In the theoretical sense "One Color", which is called "spectral line", means one wavelength (Wu,2009).

### 2.1.2.2 Directionality

This is perhaps the most obvious aspect of a laser beam: the light comes out as a highly directional beam. This contrasts with light bulbs and discharge lamps, in which the light is emitted in all directions. The directionality is a consequence of the cavity.

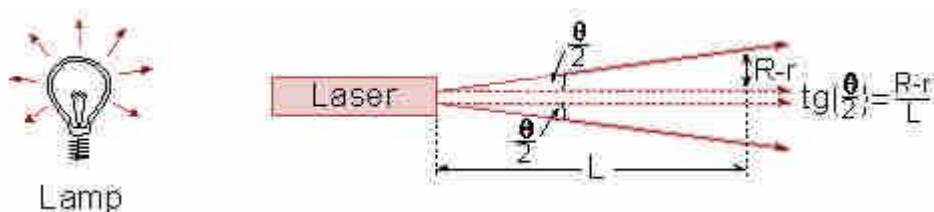


Figure 2.3 different between Laser and Lamp

Radiation comes out of the laser in a certain direction, and spreads at a defined divergence angle ( $\Theta$ ) (Wu,2009).

This angular spreading of a laser beam is very small compared to other sources of electromagnetic radiation, and described by a small divergence angle (of the order of mille-radians).

(a) From Geometric Optics point of view:

Only rays that are closely aligned with the resonator's centerline can make the required number of round trips, and these aligned rays diverge only slightly when they emerge

(b) From Wave Optics point of view:

Beam diverges due to diffraction and partial spatial coherence. The divergence of a TEM<sub>00</sub> laser beam is determined by the intrinsic size of beam within laser cavity (beam waist) (Wu,2009).

### **2.1.2.3 Brightness**

By definition Brightness is radiant flux (radiometry, power) or luminous flux (photometry) emitted per unit surface area (source) per unit solid angle. Since laser radiation divergence is of the order of milli-radians, the beam is almost parallel, and laser radiation can be sent over long distances (Wu,2009).

### **2.1.2.4 Coherence**

In discussing the coherence of an optical beam, we must distinguish between spatial and temporal coherence.

Laser beams have a high degree of both.

Temporal coherence: measure the phase correlations at different time at the same position.

Consider the electric field at a fixed point P, if there has a phase relationship between the two fields at time  $t$  and  $t+\tau$ , we say that the electric field is temporal coherence over time  $\tau$ .

If this occurs for any value  $\tau$ , the E. M wave is said to have perfect time coherence.

If this occurs for  $0 < \tau < \tau_c$ , it said to said partial temporal coherence with coherence time  $\tau_c$ .

It measures the degree of monochromaticity of the light.

In general, the temporal coherence time  $\tau_c$  is given by the reciprocal of the spectral line width.

Coherence length  $l_c = c \tau_c = \lambda^2 / \Delta\lambda = c / \Delta\nu$

Spatial coherence: measure the phase correlations at different position at the same time.

Consider P1 and P2 located on the same wave front, the distance between P1 and P2 is  $l$ . If there has a Phase relationship between the two fields at P1 and P2, for any value of  $l$ , the wave is said to have perfect spatial coherence.

In practice, P2 must lie within some finite area around P1 to have good phase relation; this wave is partial spatial coherence.

It measures the uniformity of phase across the optical wave front and depends on the length of the light source. (Wu, 2009)

## **2.2 X-rays:**

X-rays can be seen as electromagnetic waves with their associated wavelengths, or as beams of photons with associated energies. Both views are correct, but one or the other is easier to understand depending on the phenomena to be explained (Smith, 1968).

Other electromagnetic waves include light, radio waves and gamma rays, X-rays have wavelengths and energies between gamma rays and ultra violet light. The wavelengths of X-rays are in the range from 0.01 to 10 nm, which corresponds to energies in the range from 0.125 to 125 keV. The wavelength of X-rays is inversely proportional to its energy, according to  $E \times \lambda = h \times c$ . E is the energy in keV and  $\lambda$  the wavelength in nm. The term  $hc$  is the product of Planck's constant and the velocity of light and has, using keV and nm as units, a constant value of 1.23985.

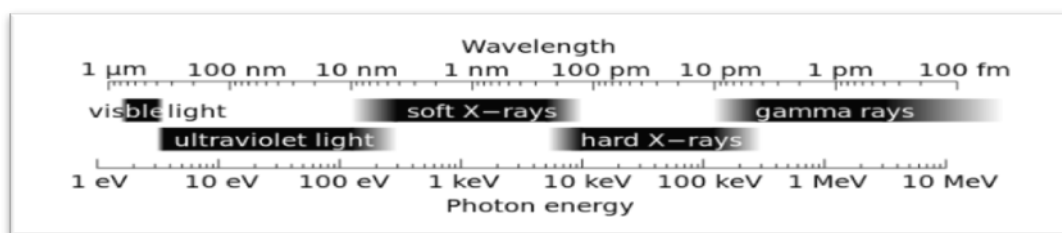


**Figure 2.4 Range of X-ray(Smith,1968).**

There are three main interactions when X-rays contact matter: Fluorescence, Compton scatter and Rayleigh scatter, if a beam of X-ray photons is directed towards a slab of material a fraction will be transmitted through, a fraction is absorbed (producing fluorescent radiation) and a fraction is scattered back. Scattering can occur with a loss of energy and without a loss of energy.

The first is known as Compton scatter and the second Rayleigh scatter. The fluorescence and the scatter depend on the thickness (d), density ( $\rho$ ) and composition of the material, and on the energy of the X-rays. The next sections will describe the production of fluorescent radiation and scatter.

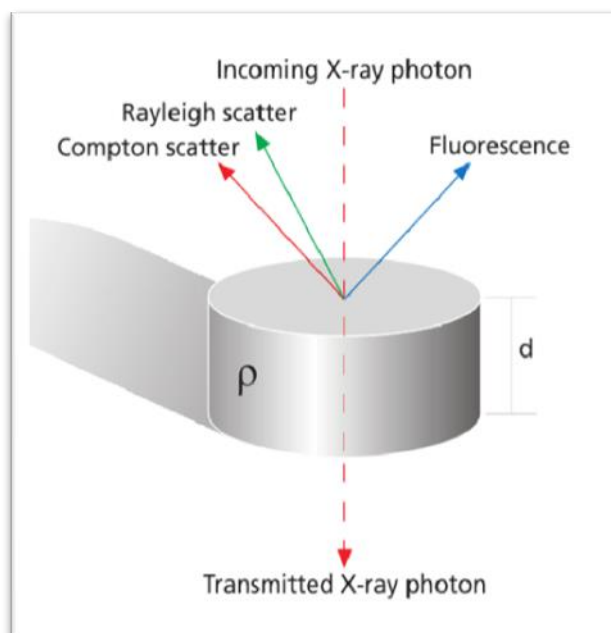


Figure 2.5 Three main interactions of X-rays with matter (Smith, 1968).

## 2.3 Spectral range

### 1-Far-infrared

The first FTIR spectrometers were developed for far-infrared range. The reason for this has to do with the mechanical tolerance needed for good optical performance, which is related to the wavelength of the light being used. For the relatively long wavelengths of the far infrared,  $\sim 10 \mu\text{m}$  tolerances are adequate, whereas for the rock-salt region tolerances have to be better than  $1 \mu\text{m}$ . A typical instrument was the cube interferometer developed at the NPL and marketed by Grubb Parsons. It used a stepper motor to drive the moving mirror, recording the detector response after each step was completed (Smith, 1968).

### 2-Mid-infrared

With the advent of cheap microcomputers it became possible to have a computer dedicated to controlling the spectrometer, collecting the data, doing the Fourier transform and presenting the spectrum. This provided the impetus for the development of FTIR spectrometers for the rock-salt region. The problems of manufacturing ultra-high precision



optical and mechanical components had to be solved. A wide range of instruments are now available commercially. Although instrument design has become more sophisticated, the basic principles remain the same. Nowadays, the moving mirror of the interferometer moves at a constant velocity, and sampling of the interferogram is triggered by finding zero-crossings in the fringes of a secondary interferometer lit by a helium–neon laser. In modern FTIR systems the constant mirror velocity is not strictly required, as long as the laser fringes and the original interferogram are recorded simultaneously with higher sampling rate and then re-interpolated on a constant grid, as pioneered by James W. Brault. This confers very high wave number accuracy on the resulting infrared spectrum and avoids wave number calibration errors (Smith,1968).

### **3-Near-infrared**

Main article: Near-infrared spectroscopy

The near-infrared region spans the wavelength range between the rock-salt region and the start of the visible region at about 750 nm. Overtones of fundamental vibrations can be observed in this region. It is used mainly in industrial applications such as process control and chemical imaging (Smith, 1968).

### **2.4 Vinasse**

One of the most important residues in the sugar crop farms that are produced from the extraction of ethanol is vinasse, which is a liquid produced by the process of fermentation of molasses for the production of alcohol and various yeasts, and has turned the attention of scientists to try to benefit from this article in many different areas for the sake of cleanliness Environment(omima,2010).

Vinasse are produced during the process of fermentation and distillation of molasses for the production of ethanol, which is produced in large quantities based on the quality of molasses ranging from 12 to 20 liters versus 1 liter of pure alcohol.

Vinasse are used after anaerobic digestion by bacteria and then burned by the large kilns to produce potassium-rich fertilizer and used for soil fertilization (omima, 2010).

**Table 2.1 showing the composition of vinasse based on wet weight (omima, 2010)**

<b>Ingredients</b>	<b>Cons %</b>
Solid	40-55
Humidity	60-45
Ash	12-18
Protein	8-15
Potassium (Potassium Oxide)	4-6.5
PH	3.5-4
Sugars	2-5

### **2.5.1 Vinasse-induced Problems**

- 1- The bad smell of the product.
- 2 - Poisoning that can be caused in case of leakage of groundwater and rivers.
- 3- Soil loses its fertility after only 5 years.

## **2.6 Nd:YAG Laser**

Nd:YAG lasers are optically pumped using a flashtube or laser diodes. These are one of the most common types of laser, and are used

for many different applications. Nd:YAG lasers typically emit light with a wavelength of 1064 nm, in the infrared. However, there are also transitions near 946, 1120, 1320, and 1440 nm. Nd:YAG lasers operate in both pulsed and continuous mode. Pulsed Nd:YAG lasers are typically operated in the so-called Q-switching mode: An optical switch is inserted in the laser cavity waiting for a maximum population inversion in the neodymium ions before it opens. Then the light wave can run through the cavity, depopulating the excited laser medium at maximum population inversion. In this Q-switched mode, output powers of 250 megawatts and pulse durations of 10 to 25 nanoseconds have been achieved.<sup>[4]</sup> The high-intensity pulses may be efficiently frequency doubled to generate laser light at 532 nm, or higher harmonics at 355, 266 and 213 nm (K.H.Wu,2009).

Nd:YAG absorbs mostly in the bands between 730–760 nm and 790–820 nm. At low current densities krypton flashlamps have higher output in those bands than do the more common xenon lamps, which produce more light at around 900 nm. The former is therefore more efficient for pumping Nd: YAG lasers (K.H.Wu,2009).

The amount of the neodymium do pent in the material varies according to its use. For continuous wave output, the doping is significantly lower than for pulsed lasers. The lightly doped CW rods can be optically distinguished by being less colored, almost white, while higher-doped rods are pink-purplish (K.H.Wu,2009).

Other common host materials for neodymium are: YLF (yttrium lithium fluoride, 1047 and 1053 nm), YVO<sub>4</sub> (yttrium orthovanadate, 1064 nm), and glass. A particular host material is chosen in order to obtain a desired combination of optical, mechanical, and thermal properties. Nd:YAG lasers and variants are pumped either by flashtubes,

continuous gas discharge lamps, or near-infrared laser diodes (DPSS lasers). Prestabilized laser (PSL) types of Nd:YAG lasers have proved to be particularly useful in providing the main beams for gravitationalwave interferometers such

as LIGO, VIRGO, GEO600 and TAMA(K.H.Wu,2009).

# CHAPTER THREE

## Experimental Part

### 3.1 Introduction

This chapter shows the material and devices and the processes that Vinasse sample were treated like burning it by Nd:YAG laser and use XRF, XRD and FT IR device to detect the sample properties.

### 3.2 Materials and Devices

#### 3.2.1 Sample of vinasse

Sample of vinasse was obtained from Kinana sugar Plantation Company.



Figure 3.1 sample of vinasse

#### 3.2.2 Nd: YAG laser Device

Use The Dornier MedilasFibertom5100 is a 100 watt Nd: YAG continuous wave laser with a 1064 nm wavelength. This versatile system is ideal for a variety of surgical applications including non-contact or interstitial coagulation, bloodless vaporization and precise tissue cutting.

The Medilas Fibertom5100also includes unique safety features including the LPS, Light guide Protection System and Fibertom cutting mode.



Figure 3.2Nd: YAG Laser,Dornier Medilas Fibertom 5100 device

### 3.2.3 X-Ray Fluorescent (XRF)



Figure 3.3 X-Ray Fluorescent device

### 3.2.3.1 Production of Fluorescent Radiation

XRF radiation is induced when photons of sufficiently high energy, emitted from an X-ray source, impinge on a material. These primary X-rays undergo interaction processes with the analyze atoms. High-energy photons induce ionization of inner shell electrons by the photoelectric effect and thus electron vacancies in inner shells (K, L, M ....) are created. The prompt transition of outer shell electrons into these vacancies within some 100  $\mu$ s can cause the emission of characteristic fluorescence radiation(Peter,2010).

Not all transitions from outer shells or sub shells are allowed, only those obeying the selection rules for electric dipole radiation. The creation of a vacancy in a particular shell results in a cascade of electron transitions, all correlated with the emission of photons with a well-defined energy corresponding to the difference in energy between the atomic shells involved. The family of characteristic X-rays from each element including all transitions allows the identification of the element.

Next to this radioactive form of relaxation, a competing process can take place: the emission of Auger electrons. Both processes have Z-dependent probabilities that are complementary: The Auger yield is high for light elements and the fluorescence yield is high for heavy elements(Peter, 2010).

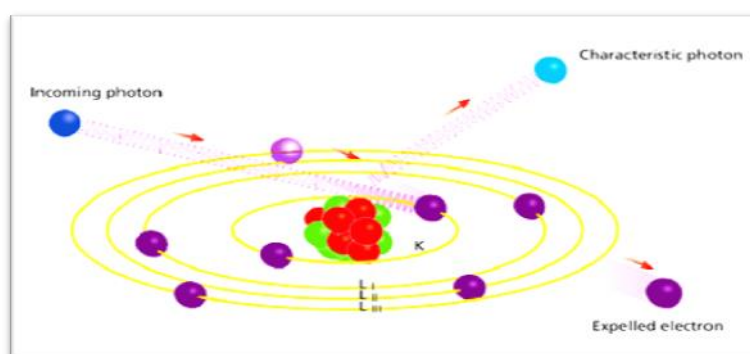


**Figure 3.4 Production of fluorinated X-ray(Peter,2010)**

### 3.2.3.2 Working Principle

The working principle of XRF analysis is the measurement of wavelength or energy and intensity of the characteristic photons emitted from the sample. This allows the identification of the elements present in the analytic and the determination of their mass or concentration all the information for the analysis is stored in the measured spectrum, which is a line spectrum with all characteristic lines superimposed above a certain fluctuating background. Other interaction processes, mainly the elastic and inelastic scattering of the primary radiation on sample and substrate, induce the background(Peter,2010).

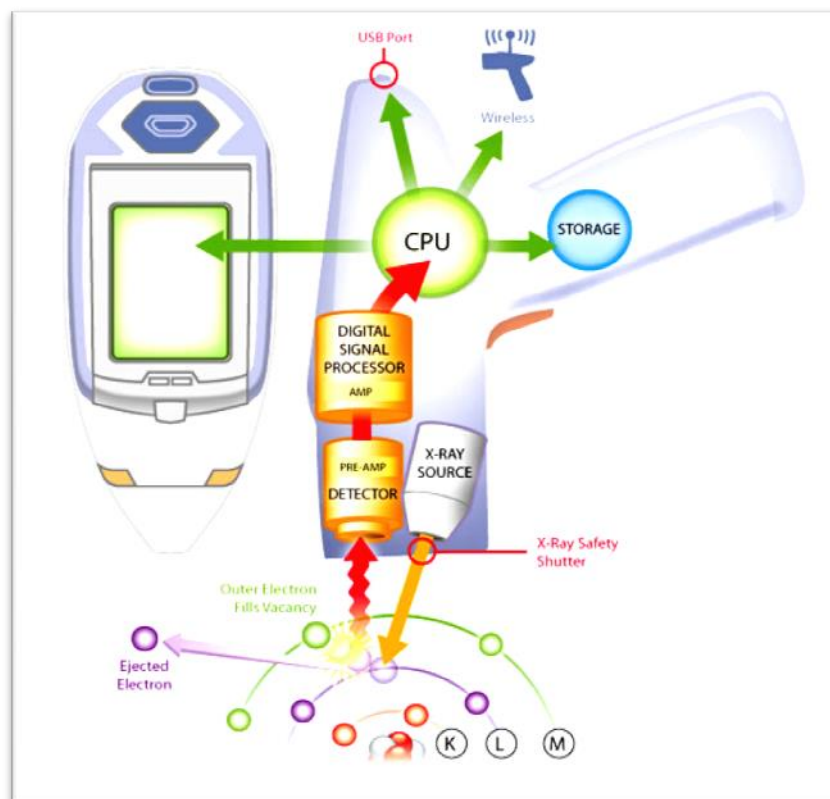


Figure 3.5a schematic diagram of the work of the machine(Peter,2010)

### 3.2.4 X-Ray Diffraction(XRD) Analysis

#### 3.2.4.1 XRD Basics

#### X-ray Generation and Properties of X-rays



X-rays are electromagnetic radiation with photon energies in the range of 100 eV - 100 keV. For diffraction applications, only short wavelength x-rays (hard x-rays) in the range of a few angstroms (Å) to 0.1 angstrom (1 keV - 120 keV) are used. X-rays are ideally suited for probing the atomic structure of solids because their wavelengths (0.1-2 Å) are of comparable length to the radii of atoms and they are sufficiently energetic to penetrate most solid materials to provide information about the bulk structure (Dr. Bruce,2006).

Most XRD instruments produce x-rays with an x-ray generating tube. In this component x-rays are generated when a focused electron beam accelerated across a high voltage field bombards a stationary solid Cu target. As electrons collide with atoms in the target and slow down, a continuous spectrum of x-rays is emitted, which is termed Bremsstrahlung radiation. The high energy electrons also eject inner shell electrons in atoms through the ionization process. When a free electron fills the shell, an x-ray photon with energy characteristic of the target material is emitted. Common targets used in x-ray tubes include Cu and Mo, that emit 8 keV and 14 keV x-rays with corresponding wavelengths of 1.54 Å and 0.8 Å, respectively. (The energy  $E$  of an x-ray photon and its wavelength ( $\lambda$ ) is related by the equation  $E = hc/\lambda$ , where  $h$  is Planck's constant and  $c$  the speed of light) (Dr. Bruce,2006).

In recent years' synchrotron facilities have become widely used as preferred sources for x-ray diffraction measurements. Synchrotron radiation is emitted by electrons or positrons traveling at near light speed in a circular storage ring. These powerful sources, which are thousands to millions of times more intense than laboratory x-ray tubes, have become indispensable tools for a wide range of structural investigations and brought advances in numerous fields of science and technology (Dr. Bruce,2006).

### 3.2.4.2 Lattice Planes and Bragg's Law

X-rays primarily interact with electrons in atoms. When x-ray photons collide with electrons, some photons from the incident beam will be deflected away from the direction where they original travel, much like billiard balls bouncing off one another. If the wavelength of these scattered x-rays did not change (meaning that x-ray photons did not lose any energy), the process is called elastic scattering (Thompson Scattering) in that only momentum has been transferred in the scattering process. These are the x-rays that we measure in diffraction experiments, as the scattered x-rays carry information about the electron distribution in materials. On the other hand, In the inelastic scattering process (Compton Scattering), x-rays transfer some of their energy to the electrons and the scattered x-rays will have different wavelength than the incident x-rays.

Diffracted waves from different atoms can interfere with each other and the resultant intensity distribution is strongly modulated by this interaction. If the atoms are arranged in a periodic fashion, as in crystals, the diffracted waves will consist of sharp interference maxima (peaks) with the same symmetry as in the distribution of atoms. Measuring the diffraction pattern therefore allows us to deduce the distribution of atoms in a material (Dr. Bruce,2006).

The peaks in an x-ray diffraction pattern are directly related to the atomic distances. Consider an incident x-ray beam interacting with the atoms arranged in a periodic manner as shown in 2 dimensions in the following illustrations. The atoms, represented as green spheres in the graph, can be viewed as forming different sets of planes in the crystal (colored lines in graph on left). For a given set of lattice plane with an inter-plane distance of  $d$ , the condition for a diffraction

(peak) to occur can be simply written as

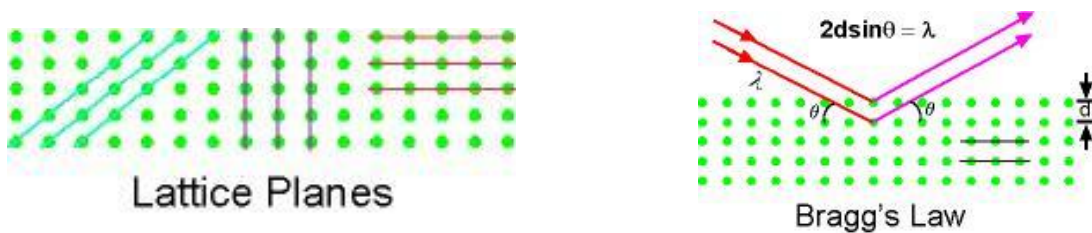


Figure 3.6 lattice planes and Bragg's law (Dr. Bruce, 2006)

$$2d\sin\Theta = n\lambda \quad (3.1)$$

Which is known as the Bragg's law, after W.L. Bragg, who first proposed it. In the equation (3.1),  $\lambda$  is the wavelength of the x-ray,  $\Theta$  the scattering angle, and  $n$  is an integer representing the order of the diffraction peak. The Bragg's Law is one of most important laws used for interpreting x-ray diffraction data. It is important to point out that although we have used atoms as scattering points in this example, Bragg's Law applies to scattering centers consisting of any periodic distribution of electron density. In other words, the law holds true if the atoms are replaced by molecules or collections of molecules, such as colloids, polymers, proteins and virus particles (Bruce, 2006).

### 3.2.4.3 Powder X-ray Diffraction

Powder XRD is perhaps the most widely used x-ray diffraction technique for characterizing materials. As the name suggests, the sample is usually in a powder form, consisting of fine grains of single crystalline material to be studied. The technique is also used widely for studying particles in liquid suspensions or polycrystalline solids (bulk or thin film materials).

The term 'powder' really means that the crystalline domains are randomly oriented in 3-D space in the sample. Therefore, when the 2-D diffraction pattern is recorded, it shows concentric rings of scattering peaks corresponding to the various  $d$  spacing's in the crystal lattice. The positions and the intensities of the peaks are used for identifying the underlying structure (or phase) of the material. For example, the diffraction lines of graphite would be different from diamond even though they both are made of carbon atoms. This phase identification is important because the material properties are highly dependent on structure (Dr. Bruce,2006).

Powder diffraction data can be collected using either transmission or reflection geometry, as shown below. Because the particles in the powder sample are randomly oriented, these two methods will yield the same data.

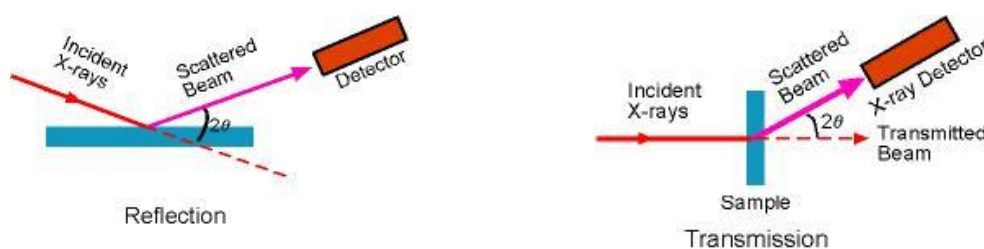


**Figure 3.7**the reflection and transmission X-Ray(Dr. Bruce,2006)

A powder XRD scan of corundum ( $\text{Al}_2\text{O}_3$ ) standard reference material provided with the D8 instrument is shown below as a plot of scattering intensity vs. the scattering angle  $2\Theta$  or the corresponding  $d$ -spacing. The peak positions, intensities, widths and shapes all provide important information about the structure of the material (Bruce, 2006).

### 3.2.5 Fourier-Transform Infrared Spectroscopy

Fourier-transform infrared spectroscopy (FTIR) is a technique used to obtain an infrared spectrum of absorption or emission of a solid,

liquid or gas. An FTIR spectrometer simultaneously collects high-spectral-resolution data over a wide spectral range. This confers a significant advantage over a dispersive spectrometer, which measures intensity over a narrow range of wavelengths at a time(Holmes,2002).

Fourier transform infrared spectroscopy technique is used for the determination of the functional groups responsible for the sorption process. Adsorption in the infrared region occurs due to vibrational and rotational motions giving rise to stretching and bending of molecular groups (Barakat,2011).

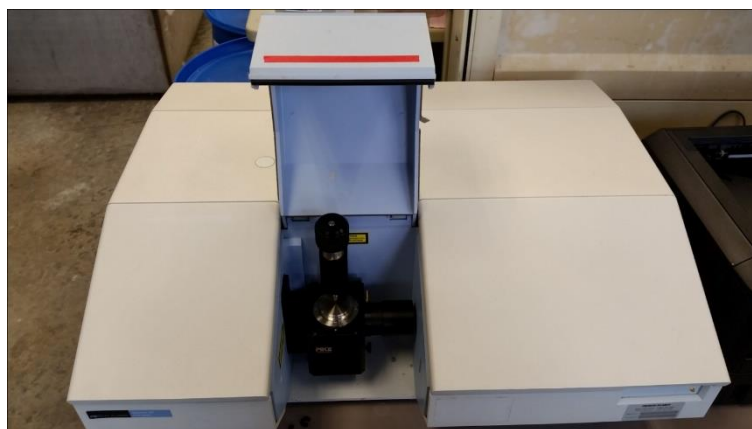


**Figure 3.8** An example of an FTIR spectrometer with an attenuated total reflectance (ATR) attachment(Barakat,2011)

### **3.3 Method**

Vinasse sample was placed into a high-temperature glass beaker (Schott Duran—Germany) and it was burned on the air by the heat of Nd: YAG laser (Dornier Medilas fiber to 5100) with an output power of 60 W for 30 s. The laser beam was delivered by single mode fiber optic with diameter 125  $\mu\text{m}$ , the distance between the sample and the end of the fiber optic was 1 cm. Because of the small spot size of the laser beam, the process of burning was done point by point, the laser was fixed on a holder while the high-temperature glass beaker was rotated

every 30 s carefully for approximately 5 mm, this step repeated many times before investigations for accuracy.

# CHAPTER FOUR

## Result and Discussion

### 4.1 introduction

This chapter shows the results of the characterization of vinasse samples like Ray fluoresce analyze, X-Ray Diffraction and FTir analyze and discussion this result.

### 4.2 Result and Discussion

#### 4.2.1 FTIR Result

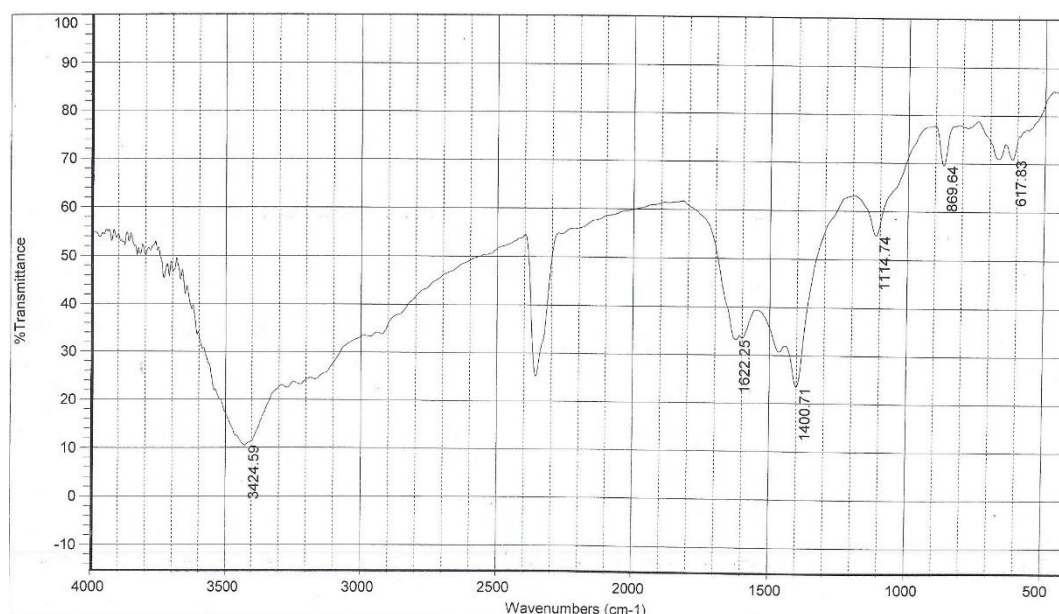


Figure 4.1 FT-IR analysis result

In the FT-IR analysis found functional C-H stretching in beak 617.83 cm<sup>-1</sup> (MakawaTafadzwa,2016), FeFeOH in beak 869.64 cm<sup>-1</sup> (Goodman et al, 1976), SiO-Si stretching in beak 1114.74 cm<sup>-1</sup> (Moenke, 1974), Na<sub>2</sub>CO<sub>3</sub>in beak 1400.71 cm<sup>-1</sup> (Moreno,2002) and stretching vibrations of -C=N in beak 1622.25cm<sup>-1</sup>(Jingwei Zheng, Lin Ma,2015).

**Table 4.1 show the result of FT-IR analyze**

<b>FTir shift</b>	<b>Functional</b>	<b>Reference</b>
617.83	C-H stretching	(MakawaTafadzwa,2016)
869.64	FeFeOH	(Goodman et al, 1976)
1114.74	SiO-Si stretching band	(Moenke, 1974)
1400.71	Na <sub>2</sub> CO <sub>3</sub>	(Moreno,2002)
1622.25	stretching vibrations of -C=N	(Jingwei Zheng, Lin Ma,2015)

#### **4.2.2XRF analyze**

**Table 4.2 XRF analyze after burning**

<b>Analyze Element</b>	<b>Conc.</b>	<b>STD</b>
Cr	0.06%	0.020
Mn	0.00%	0.008
Fe	0.27%	0.028
Ni	0.01%	0.002
Cu	0.00%	0.003
Zn	0.00%	0.002
Pb	0.00%	0.003



In XRF analyze was found some elements like Chrome by 0.06%, Iron by 0.27% and Nickle by 0.01% and wasn't found some elements like Manganese,Zinc, Copper and Lead by this result confirmed FTIR result as found as functional of iron but this analytic just search for 7 elements.

### 4.2.3 XRD Analyzing

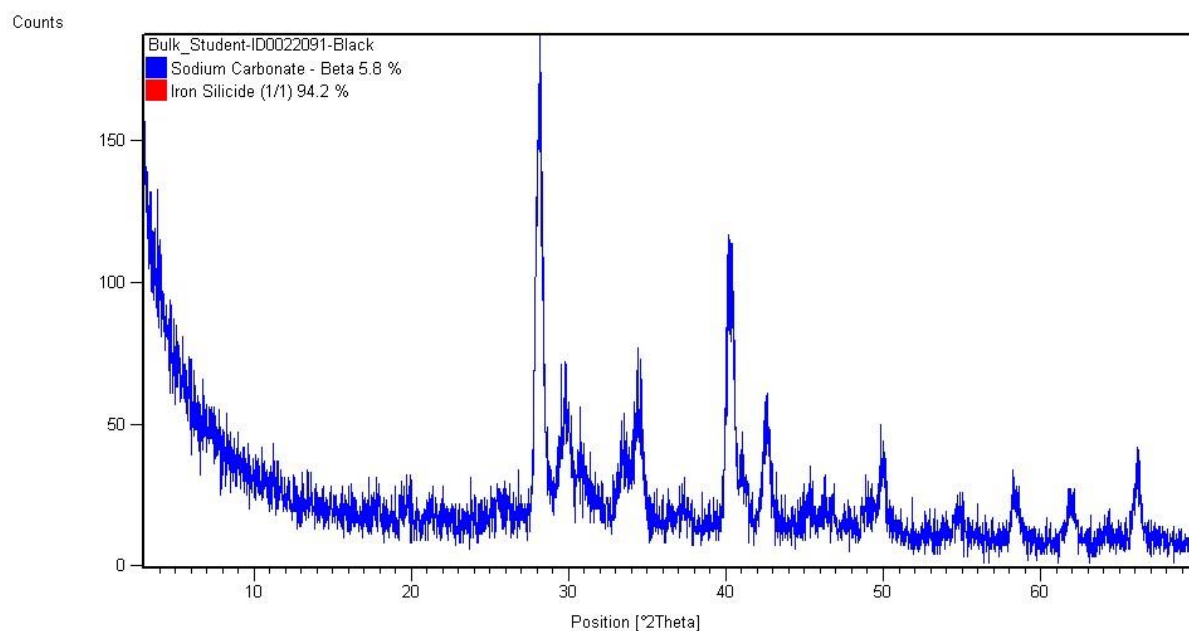


**Figure 4.2 XRD analyze**

In the XRD analyze found tow subject iron silicide (1/1) by 94.2% and Sodium Carbonate-Beta by 5.8% this analytic confirmed the FTIR analysis because it proved the presence of iron functional and sodium carbonate.

### 4.3 Conclusions

From this result we can say that the resulting material is rich from sodium carbonate and iron silicide as that proved by the FTIR analysis which confirmed the existence of a number of functional groups (C-H stretching, Fe-OH, SiO-Si stretching band,  $\text{Na}_2\text{CO}_3$ , stretching vibrations of  $\text{C}=\text{N}$ ) in which the XRF test confirmed the existence of a group iron and confirmed XRD where it rich material of sodium carbonate and iron silicide in the many numbers of Miller

### 4.4 Recommendations

1. The iron silicide exhibits metallic, semiconductor, or insulating behavior depending on their structure. In future studies, preparation of nano-particle could be investigated by this method.
2. Vinasse material could be used to prepare Sodium Carbonate and iron silicide.
3. This analysis isn't enough to a proof the material is just have this element so we can use more analysis ICP analyze .
4. Need to use analyze can found the potassium .

## References

- Barakat, M. 2011."New trends in removing heavy metals from industrial wastewater," *Arabian Journal of Chemistry*, 4, pp. 361–377.
- Brouwer, P., 2006. *Theory of XRF. Almelo, Netherlands: PANalytical BV.*
- Dr. Omaima Mohamed Sawan, Dr. Mahmoud Helmy Mostafa. 2010. *Evidencerecycling of agricultural wastes.*
- Goodman, B. A., Russell, J. D., Fraser, A. R., &Woodhams, F. W. D. 1976. A Mössbauer and IR spectroscopic study of the structure of nontronite. *Clays and Clay Minerals*, 24(2), 53-59.
- Griffiths, P.R. and De Haseth, J.A., 2007. *Fourier transform infrared spectrometry* (Vol. 171). John Wiley & Sons.
- Griffiths, P.R.; Holmes. 2002. *Handbook of Vibrational Spectroscopy, Vol 1.* Chichester : John Wiley and Sons
- Ichimura, A. and Manning, B., 2004. *Bruker D8 ADVANCE Powder XRD Instrument Manual and Standard Operating Procedure (SOP).* *San Francisco State University, August.*
- Prof. K. H.Wu .2009 .*Fundamental Optics*
- Smith, D.R., Morgan, R.L. and Loewenstein, E.V., 1968. Comparison of the radiance of far-infrared sources. *JOSA*, 58(3), pp.433-434.
- Makawa, T. 2016. Adsorptive potential of maize tassel-ethyl acrylate biopolymer embedded magnetic nanohybrid towards the removal

of cd (ii) from aqueous solution: An experimental design methodology.

Moenke, H. H. W. 1974. Silica, the three-dimensional silicates, borosilicates and beryllium silicates. Infrared spectra of minerals.

M.C.M.M.Moreno.2002 . FT-IR Quantitative Analysis of Calcium Carbonate (Calcite) and Silica (Quartz) Mixtures Using the Constant Ratio Method . Application to Geological Samples .Talanta

Zheng, J., &Ma, L. 2015. Silver (I) complexes of 2, 4-dihydroxybenzaldehyde–amino acid Schiff bases—Novel noncompetitive  $\alpha$ -glucosidase inhibitors. Bioorganic & medicinal chemistry letters, 25(10), 2156-2161.

## Appendix

Table show Miller coordinates of Sodium Carbonate-Beta was found in subject

H	k	L	Assignment
0	0	1	Sodium Carbonate – Beta
2	0	0	Sodium Carbonate – Beta
1	1	0	Sodium Carbonate – Beta
2	0	-1	Sodium Carbonate – Beta
1	1	-1	Sodium Carbonate – Beta
2	0	1	Sodium Carbonate – Beta
1	1	1	Sodium Carbonate – Beta
0	0	2	Sodium Carbonate – Beta
2	0	-2	Sodium Carbonate – Beta
3	1	0	Sodium Carbonate – Beta
1	1	-2	Sodium Carbonate – Beta
0	2	0	Sodium Carbonate – Beta
1	1	2	Sodium Carbonate – Beta
2	0	2	Sodium Carbonate – Beta
3	1	-1	Sodium Carbonate – Beta
3	1	1	Sodium Carbonate – Beta
0	2	-1	Sodium Carbonate – Beta
0	2	1	Sodium Carbonate – Beta
4	0	0	Sodium Carbonate – Beta
2	2	0	Sodium Carbonate – Beta
4	0	-1	Sodium Carbonate – Beta
2	2	-1	Sodium Carbonate – Beta
4	0	1	Sodium Carbonate – Beta
2	2	1	Sodium Carbonate – Beta
0	0	3	Sodium Carbonate – Beta
3	1	-2	Sodium Carbonate – Beta
0	2	2	Sodium Carbonate – Beta
0	2	-2	Sodium Carbonate – Beta
3	1	2	Sodium Carbonate – Beta
2	0	-3	Sodium Carbonate – Beta
1	1	-3	Sodium Carbonate – Beta
1	1	3	Sodium Carbonate – Beta
2	0	3	Sodium Carbonate – Beta
4	0	-2	Sodium Carbonate – Beta
2	2	-2	Sodium Carbonate – Beta
4	0	2	Sodium Carbonate – Beta
2	2	2	Sodium Carbonate – Beta
4	0	2	Sodium Carbonate – Beta
2	2	2	Sodium Carbonate – Beta
5	1	0	Sodium Carbonate – Beta
4	2	0	Sodium Carbonate – Beta
1	3	0	Sodium Carbonate – Beta
5	1	-1	Sodium Carbonate – Beta

3	1	-3	Sodium Carbonate – Beta
4	2	-1	Sodium Carbonate – Beta
5	1	1	Sodium Carbonate – Beta
4	2	1	Sodium Carbonate – Beta
1	3	-1	Sodium Carbonate – Beta
0	2	-3	Sodium Carbonate – Beta
0	2	3	Sodium Carbonate – Beta
1	3	1	Sodium Carbonate – Beta
3	1	3	Sodium Carbonate – Beta
0	0	4	Sodium Carbonate – Beta
4	0	-3	Sodium Carbonate – Beta
2	2	-3	Sodium Carbonate – Beta
2	2	3	Sodium Carbonate – Beta
4	0	3	Sodium Carbonate – Beta
2	2	3	Sodium Carbonate – Beta
5	1	-2	Sodium Carbonate – Beta
4	2	-2	Sodium Carbonate – Beta
6	0	0	Sodium Carbonate – Beta
2	0	-4	Sodium Carbonate – Beta
3	3	0	Sodium Carbonate – Beta
1	3	-2	Sodium Carbonate – Beta
1	1	-4	Sodium Carbonate – Beta
5	1	2	Sodium Carbonate – Beta
1	3	2	Sodium Carbonate – Beta
4	2	2	Sodium Carbonate – Beta
1	1	4	Sodium Carbonate – Beta
2	0	4	Sodium Carbonate – Beta
6	0	-1	Sodium Carbonate – Beta
6	0	1	Sodium Carbonate – Beta
3	3	-1	Sodium Carbonate – Beta
3	3	1	Sodium Carbonate – Beta
6	0	-2	Sodium Carbonate – Beta
3	1	-4	Sodium Carbonate – Beta
3	3	-2	Sodium Carbonate – Beta
6	0	2	Sodium Carbonate – Beta
0	2	-4	Sodium Carbonate – Beta
0	2	4	Sodium Carbonate – Beta
3	3	2	Sodium Carbonate – Beta
4	2	-3	Sodium Carbonate – Beta
3	1	4	Sodium Carbonate – Beta

**Table 4.2 show Miller coordinates of iron silicide was found on subject**

h	K	L	Assignment
0	1	1	Iron Silicide (1/1)
1	1	1	Iron Silicide (1/1)
0	1	2	Iron Silicide (1/1)
0	2	1	Iron Silicide (1/1)
1	1	2	Iron Silicide (1/1)
0	2	2	Iron Silicide (1/1)
0	1	3	Iron Silicide (1/1)
0	3	1	Iron Silicide (1/1)
1	2	2	Iron Silicide (1/1)

